Imaging Intracranial Vessel Wall Pathology With Magnetic Resonance Imaging

Current Prospects and Future Directions

Nikki Dieleman, MSc; Anja G. van der Kolk, MD; Jaco J.M. Zwanenburg, PhD; Anita A. Harteveld, MSc; Geert J. Biessels, MD, PhD; Peter R. Luijten, PhD; Jeroen Hendrikse, MD, PhD

To date, the probable cause of ischemic stroke is often inferred from the size and location of the infarct, in combination with an evaluation of the heart and the presence of extracranial arterial occlusion or high-grade stenosis.[1] Currently used conventional lumenography-based methods such as digital subtraction angiography, computed tomography angiography, and magnetic resonance (MR) angiography are used to determine the presence of such an acute occlusion or high-grade arterial stenosis. From extracranial studies, it is known that luminal narrowing may be absent in patients with severe atherosclerosis owing to arterial remodeling.[2–4] Therefore, these methods do not provide information about the underlying pathological processes, which most often involve the vessel wall.[5] Vessel wall changes such as vessel wall thickening, enhancement, or the presence of vulnerable atherosclerotic plaques without luminal stenosis are therefore often missed but might be of importance for a better understanding of ischemic stroke.[6] Furthermore, intracranial atherosclerosis is an important cause of ischemic stroke[7] and often involves the vessel wall. Patients with intracranial atherosclerosis have high recurrent stroke rates,[8] and increasingly more attention is being directed to the assessment of the intracranial vessel wall, necessitating an imaging technique directly assessing the intracranial vessel wall. MR imaging (MRI) seems the most promising technique to reliably image intracranial vessel wall pathologies because of its superior soft tissue contrast. Recent advances in MRI[9] have made it possible to obtain information about these abnormalities within the intracranial vessel wall, which provides an imaging tool to investigate the role of intracranial vessel wall abnormalities in the diagnosis of stroke.

In this review, we discuss the current status of intracranial vessel wall MRI and its potential to identify different intracranial vessel wall pathologies. First, we present the state-of-the-art MRI methods to visualize the intracranial vessel wall and its pathology and we provide the technical background of these imaging methods. This part also focuses on imaging at different field strengths and on healthy vessel wall and different wall pathologies. Then, we give an overview of intracranial vessel wall abnormalities that may be expected for each ischemic stroke subtype. Finally, given the clinical needs and technical possibilities, we review the future clinical and technical directions of intracranial vessel wall imaging and provide a tentative recommendation for use in daily clinical practice.

MRI of Intracranial Vessel Wall Pathology

Technical Requirements

To successfully image the intracranial vessel wall, MRI methods have been developed and optimized that suppress the intracranial arterial blood signal and, in some cases, combine this with suppression of the cerebrospinal fluid (CSF) signal around the intracranial arteries proximally and distally of the circle of Willis.[9–22] Obtaining black-blood signal for all intracranial arteries is essential for sufficient image contrast to assess the vessel wall and its pathology. The distal internal carotid arteries, distal vertebral arteries, and basilar artery have a predominant caudal-cranial course, which may be beneficial when the outflow of blood is used together with a transverse imaging plane perpendicular to the arteries proximally of the circle of Willis. The basilar artery especially has been shown to be well suited for vessel wall imaging because of its relative large size and straight course.[20] On the other hand, compared with the arteries in the neck, the anterior, middle, and posterior branches of the circle of Willis all have a different course, and black-blood imaging based on outflow may be more difficult. Some of the black-blood imaging methods that have been developed for the neck may also be applied and optimized for intracranial vessel wall imaging. These black-blood techniques include double inversion recovery[23] and techniques that are based on motion-sensitizing prepulses.[24,25] A disadvantage might be that slow flow next to the vessel wall results in incomplete blood suppression, thereby overestimating vessel wall thickness.[26]

For the detection of focal thickening of the intracranial vessel walls, signal suppression on the outside of intracranial vessel walls is a prerequisite. Most of the intracranial arteries are surrounded by CSF. In elderly patients, this amount of

From the Department of Radiology (N.D., A.G.v.d.K., J.J.M.Z., A.A.H., P.R.L., J.H.), Image Sciences Institute (J.J.M.Z.), and Department of Neurology (G.J.B.), University Medical Center Utrecht, Utrecht, the Netherlands.

Correspondence to Nikki Dieleman, Department of Radiology, Room E01.132, University Medical Center Utrecht, PO Box 85500, 3508 GA, Utrecht, The Netherlands. E-mail n.dieleman@umcutrecht.nl

(*Circulation*. 2014;130:192-201.)

***Circulation* is available at http://circ.ahajournals.org** **DOI: 10.1161/CIRCULATIONAHA.113.006919**

Table 1. Scan Parameters Used in Studies Assessing Intracranial Vessel Wall Pathology With MRI

Field Strength, T	MRI	Authors	Scan Duration, Minimum–Maximum, min	FOV, Minimum–Maximum, mm	Resolution, Minimum–Maximum, mm	TR/TE/TI, ms	Pulse Sequence	Contrast Enhancement
1.5	T1-weighted imaging	Aoki et al[27]	2.24–12.00	150×150×3.0	0.6×0.7×2.0	600/15	SE	+
		Aoki et al[28]		150×150×3.0	0.6×0.7×2.0	400–600/8–15	SE	+
		Klein et al[29]		120×120×2-3	0.4×0.5×2.0	900/15	FSE	+
		Park et al[13]		150×150×3.0	0.48×0.58×2.0	n.g.	n.g.	–
		Küker et al[30]		n.g.	n.g.	n.g.	n.g.	+
		Natori et al[31]		250×190×190	0.5×0.5×0.5	500/18.3	FSE	–
		Vakil et al[32]		220×240×5.0	0.9×0.9×5.0 (gap 1.5)	663/15	SE	+
1.5	T2-weighted imaging	Aoki et al[28]	11.20–12.00	150×150×3.0	0.6×0.7×2.0	3000–4000/80–100	(F)SE	–
		Klein et al[29,33,34]		120×120×2.5	0.4×0.5×2.0–0.4×0.4×2.5	3500/70	FSE	–
		Küker et al,[30] Park et al[13]		150×150×3.0	0.48×0.58×2.0	n.g.	TSE	–
1.5	PD-weighted imaging	Aoki et al[28]	7.47	150×150×3.0	0.6×0.7×2.0	2000–4000/14–30	SE	–
		Klein et al[29,33]		120×120×2.5	0.4×0.5×2.0–0.4×0.4×2.5	1500–2600/15	FSE	+
1.5	Dual-echo images	Lam et al[35]	3.41–4.15	200×200×3.0	0.8×0.8×3.0	3000/120	FSE	–
		Chen et al[36]*		170×170×3.0	0.9×0.7×3.0	3000/19–130	TSE	–
1.5	Balanced fast field echo	Sparing et al[37]		220×220×1.4	0.4×0.4×1.4	5.6/2.8	FSE	–
3	T1-weighted imaging	Chung et al[14]	2.88–11.38	100×125×2.0	0.4×0.6×2.0	700/23	TSE	–
		Chung et al[38]		100×100×1.0	0.5×0.5×1.0	800–100/8.4	TSE	+
		Lou et al,[10] Ma et al[11]		160×160×2.0	0.6×0.5×2.0	800/8.6	FSE	+
		Mandell et al[18]		220×220×2-3	0.4×0.4×2-3	2263/13/860	FSE	+
		Matouk et al[39]		160×160×2.0	0.3×0.3×2.0	590/10	TSE	+
		Pfefferkorn et al,[19] Saam et al[22]		200×200×2.0	0.4×0.4×2.0	800/13	TSE	+
		Ryu et al[21]		120×105×2.0	0.4×0.5×2.0	581/20	TSE	–
		Shi et al[40]		80×80×2.0	0.3×0.3×2.0	700/14	TSE	–
		Skarpathiotakis et al,[41] Swartz et al[42]		160×220×2.0	0.4×0.6×2.0	2108/12/860	FSE	+
		Swartz et al[42]		160×220×3.0	0.4×0.6×3.0	450/21	SE	+
		Turan et al[43]		128×128×128	0.4×0.4×1.2	458/16	TSE	+
		Turan et al[43]		100×100×100	0.4×0.4×1.2	2500/14/140	TSE	–
		Xu et al[44,45]		130×130×2.0	0.5×0.5×2.0	800/12	DIR	–
		Vergouwen et al[46,47]		n.g.	n.g.	n.g.	n.g.	+
3	T2-weighted imaging	Chung et al[14]	3.20–6.87	100×125×2.0	0.4×0.6×2.0	1800/78	TSE	–
		Chung et al[38]		100×100×1.0	0.5×0.5×1.0	2000/100	TSE	–
		Li et al,[48] Xu et al[45]		130×130×2.0	0.5×0.5×2.0	3000/50	FSE	–
		Ma et al[11]		160×160×2.0	0.6×0.5×2.0	3000/12.5	FSE	–
		Niizuma et al[49]		120×120×2.0	0.2×0.5×2.0	2800/50.8	FSE	–
		Ryu et al[21]		120×105×2.0	0.4×0.5×2.0	3000/80	TSE	–
		Shi et al[40]		140×140×0.6	0.6×0.6×0.6	2500/67	TSE	–

(*Continued*)

Table 1. Continued

Field Strength, T	MRI	Authors	Scan Duration, Minimum–Maximum, min	FOV, Minimum–Maximum, mm	Resolution, Minimum–Maximum, mm	TR/TE/TI, ms	Pulse Sequence	Contrast Enhancement
		Skarpathiotakis et al,[41] Swartz et al[42]		160×220×2.0	0.3×0.4×2.0	3450/92	FSE	–
		Turan et al[43]		104×104×104	0.4×0.4×1.2	1500/66	TSE	–
		Vergouwen et al[47]		n.g.	n.g.	n.g.	n.g.	–
3	PD-weighted imaging	Chung et al[14]	3.20–9.17	100×125×2.0	0.4×0.6×2.0	1800/26	TSE	–
		Chung et al[38]		100×100×1.0	0.5×0.5×1.0	2000/32	TSE	–
		Kim et al,[15,16] Ryu et al[21]		120×105×2.0–120×110×2.0	0.4×0.5×2.0	2500/30	TSE	–
		Kim et al[17]		104×120×1.0	0.3×0.5×1.0	3000/30	TSE	–
		Kim et al[17]		105×120×1.0	0.4×0.6×1.0	2000/40	TSE	–
		Ma et al[11,12]		160×160×2.0	0.6×0.5×2.0	3000/12.5	FSE	–
		Qiao et al[20]		200×166×45	0.5×0.5×0.5	2000/38	TSE	–
		Qiao et al[20]		120×90×2.0	0.25×0.25×2.0	200/38	TSE	–
		Shi et al[40]		80×80×2.0	0.3×0.3×2.0	2400/17	TSE	–
		Zhu et al[50]		160×160×2.0	0.6×0.6×2.0	4000/12.9	FSE	–
3	T1-weighted MRDTI	Turan et al[51]	9	320×320×224	0.7×0.7×0.7	8.7/3.8	GE	–
7	T1-weighted MPIR TSE	van der Kolk et al[9]	12	220×180×13	0.8×0.8×0.8	6050/23/1770	TSE	+
	Mixed contrast T1+T2	Majidi et al[53]*	453	95×119×10.4	0.13×0.13×0.13	3000/60	TSE	–

FOV indicates field of view; FSE, fast spin echo; MPIR, magnetization preparation inversion recovery; MR, magnetic resonance; MRDTI, magnetic resonance direct thrombus imaging; n.g., not given; PD, proton density; SE, spin echo; TE, echo time; TI, inversion time; TR, repetition time; and TSE, turbo spin echo.

*Specimen studies.

CSF surrounding the intracranial arteries increases as a result of brain atrophy.[9] With MRI methods that provide dark CSF signal or suppress the CSF signal, the outer walls will become visible (Table 1). A combination of intracranial methods that suppress the blood and the CSF will result in the visualization of both the inner and outer arterial vessel wall. However, suppressing the CSF will cost signal-to-noise ratio (SNR) within the vessel wall, and there may be a time penalty for the optimization of MRI methods. Especially when these methods are combined with high-spatial-resolution imaging, scan times may become too long.[49]

Because the diameter of the intracranial arteries is very small, ranging from 2 to 3 mm proximally to <1 mm more distally,[9,54,55] sufficient SNR and, concordant to that, submillimeter spatial resolution are required to allow the detection of vessel wall changes such as plaques, vessel wall thickening, and focal enhancement. Especially for vessel wall imaging of the arteries distal to the circle of Willis, a high spatial resolution is needed.[9,42] To obtain such a high resolution within clinically reasonable scan times, scan coverage has to be reduced (Table 1). Most current intracranial vessel wall imaging methods therefore visualize only a relatively small portion of the intracranial arteries and focus on arteries at the level of the circle of Willis and just proximal to it.[10–12,14–17,21,40,44,45,49,50] Smaller distal intracranial arterial vessel walls are beyond the scope of these sequences.[42] However, a relatively low spatial resolution may well be sufficient to detect enhancement of a lesion or more generalized enhancement of the intracranial vasculature as a result of an increase in contrast-to-noise ratio caused by the contrast uptake (Table 1).[27,28,30] Third, not only the in-plane resolution but also, in the case of 2-dimensional sequences, slice thickness is of importance. When the slice orientation is perpendicular to the artery of interest, the slice can be relatively thick. Still, when different segments with variable orientations to the intracranial arteries need to be assessed, multiple 2-dimensional slices need to be scanned, with each slice oriented perpendicular to the local vessel orientation. In this case, a 3-dimensional sequence with isotropic resolution may be superior because of its reconstruction possibilities that allow reconstruction of image planes perpendicular to the local vessel orientation afterward. The currently available MRI methods use different resolutions and slice thicknesses (Table 1), and the images are often acquired at a lower spatial resolution with the use of interpolation by zero filling during reconstruction to view the images at a higher resolution.[44,45,50] Although zero filling may yield a smoother visualization of the vessel walls, the acquired resolution determines the actual available information of the vessel wall lesions.

Magnetic Field Strength

To image the thin intracranial vessel wall at a high resolution, high SNR is essential. To obtain acceptable SNR, one can

move to higher field strengths because SNR scales linearly with field strength.[9,56] The gain in SNR can, in principle, be used for either a shorter scan time or a higher spatial resolution compared with lower field strengths.[52] Because this will allow higher spatial resolution within a reasonable scan time, intracranial vessel wall imaging is performed mainly at higher field strengths nowadays (Table 1). The first studies of intracranial vessel wall imaging were performed at a field strength of 1.5 T (Table 1). Because of the lower achievable spatial resolution of these scanners for sufficient SNR, most interest was paid to intracranial vessel wall lesions with a high contrast-to-noise ratio (Table 1) such as vividly enhancing lesions of intracranial arterial walls caused by cerebral vasculitis. With the availability of clinical 3 T MRI scanners, smaller lesions that were typically below the detection limit of 1.5 T MRI became detectable. At 3 T, intracranial vessel wall imaging showed the presence of intracranial plaques and enhancement of intracranial lesions.[10–14,21,33-35,40,44,45–49] Most of these lesions were first described in the posterior circulation (distal vertebral and basilar artery),[10–12,16,29,34,38] whereas more recent studies also showed these abnormalities in the middle cerebral arteries.[13–15,17,21,29,31,35,36,40,44,45–49,57] In the last decade, 7 T MRI scanners have become available in a number of research centers and hospitals worldwide. With the even higher attainable SNR at 7 T, it became possible to perform isotropic vessel wall imaging with a larger coverage both in vivo[9] and ex vivo[53] (Table 1). This made it possible to reconstruct each artery with a different course in different orientations without the loss of detail (Figure 1).[9] Pulse sequence optimization at the various field strengths may even allow more detail, for instance, characterization of vessel wall lesions and visualization of more peripherally located arteries. The developments and optimization of vessel wall imaging protocols at higher field strengths (7 and 3 T) may teach us disease-specific key imaging findings of the intracranial arterial walls at high resolution. Head-to-head comparison studies are currently not available but should be performed in the future to examine the appropriate imaging method and MRI field strength for the detection and characterization of intracranial vessel wall lesions.

Healthy Vessel Wall

Imaging vessel wall pathology has been shown to be easier than imaging the thinner, normal, healthy vessel wall. The latter clearly requires a higher resolution and good contrast both between the inner side of the arterial vessel wall and the blood and between the outer vessel wall and the CSF (Figure 2).[9] In young patients with limited brain atrophy, the outer vessel wall of the more distal intracranial arteries may be located next to the brain parenchyma, and CSF suppression alone might not be sufficient to show the outer wall of these arteries.[9] Visualization of the thicker vessel walls of the intracranial vessels proximal to the circle of Willis and the proximal middle cerebral artery may be easier compared with more distal, very thin vessel walls of small vessels such as the distal middle cerebral artery and the posterior and anterior cerebral arteries. In clinical practice, the healthy vessel wall was shown to be rather difficult to depict with the currently available imaging methods.[9,20,21,27,42,44,45,48] However, visualization of the healthy intracranial vessel wall may be important for several reasons. First, pathological changes in the vessel wall, especially when nonfocal pathology is concerned, may be discovered only when a comparison is made between the possible pathological vessel wall and its healthy contralateral side. Second, similar to the intima-media thickness measurements of the carotid artery,[58] clear visualization of the intracranial arterial walls may allow thickness measurements of these vessel walls, even when no pathological process is present. Thickness measurements of the intracranial vessel walls may serve as a general parameter or biomarker for the status of these intracranial arteries, as for the carotid artery.[59] At this moment, however, this is not yet feasible; at least 2 voxels within the vessel wall are needed for dedicated measurements; therefore, an in-plane resolution of ≤0.2 mm is required. Third, clear visualization of the arterial vessel walls, together with the presence of atherosclerotic changes and focal plaques, may allow the assessment of possible arterial remodeling with a widening of the arterial diameter at the location of the plaque.[4] On the other hand, the resolution and contrast-to-noise ratio required to visualize the healthy vessel wall may increase the scan time for the vessel wall imaging sequence to a degree that this method cannot be easily added to a standard clinical MRI examination. On the basis of the indication of intracranial vessel wall imaging, the methods may be optimized to focus on visualization of focal plaques and enhancement of vessel walls rather than clear visualization of the healthy vessel walls.

Nonenhancing Vessel Wall Lesions

When intracranial vessel wall lesions are evident, they may be visualized with intracranial vessel wall

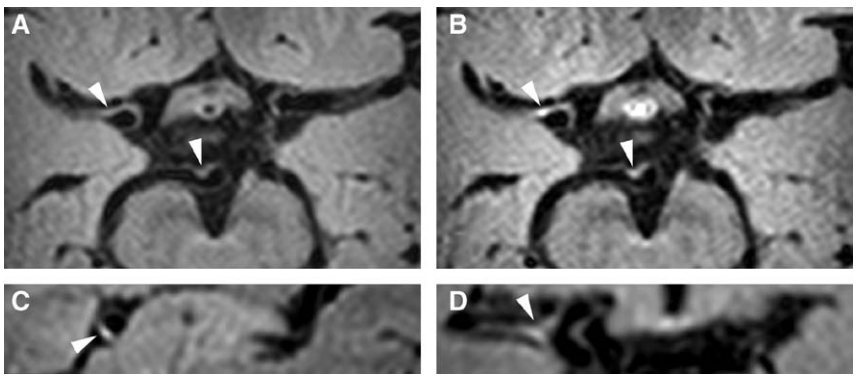

Figure 1. A 58-year-old man presented with transient hemiparesis of the left arm and leg caused by transient ischemic attack of the right middle cerebral artery. The 7 T 3-dimentional magnetization preparation inversion recovery turbo spin-echo transverse images before (**A**) and after (**B**) contrast administration show a focal atherosclerotic lesion of the right M1 branch just after its bifurcation and a lesion in the distal basilar artery, both enhancing after contrast administration (**arrowheads**). **C** and **D**, Sagittal and coronal reconstructions of the contrast-enhanced focal lesion of the right M1 branch.

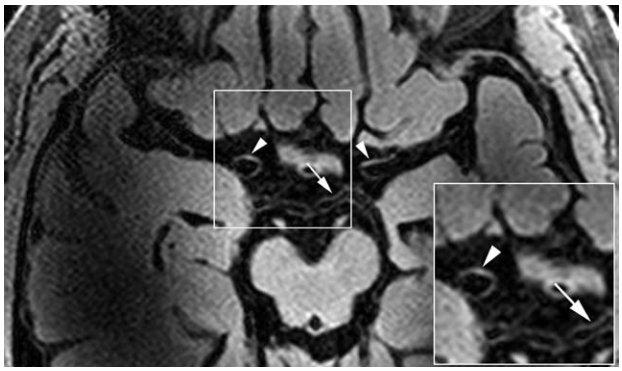

Figure 2. A 79-year-old man with a history of transient ischemic attacks of the right hemisphere presented with dysphasia and a right-sided facial paralysis resulting from a small cortical ischemic stroke of the frontal part of the middle cerebral artery territory as seen on diffusion-weighted magnetic resonance images (not shown). A 7 T transverse 3-dimensional magnetization preparation inversion recovery turbo spin-echo image with zoomed box, before contrast administration, shows smooth, healthy vessel wall (**arrows**) and thickening of the left and right M1 branch (**arrowheads**) probably of atherosclerotic origin.

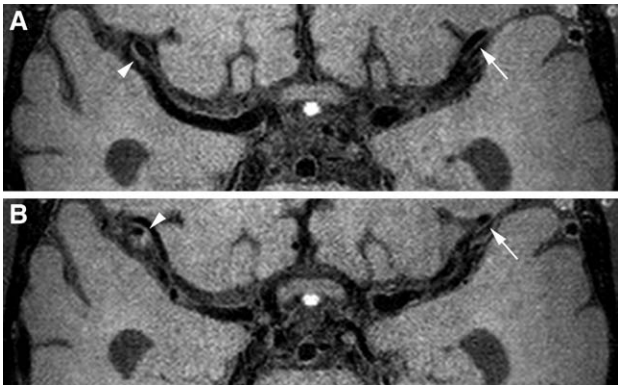

Figure 3. A 63-year-old man presented with aphasia resulting from infarctions of the left and right middle cerebral artery territory and a cerebral hemorrhage in the left hemisphere as seen on diffusion-weighted magnetic resonance and fluid-attenuated inversion-recovery images (not shown) suspected of having cerebral vasculitis. **A** and **B**, Postcontrast 3 T 3-dimensional T1-weighted volumetric isotropic turbo spin-echo acquisition (sequence adjusted from Qiao et al;[20] repetition time/echo time, 1500/35 milliseconds) vessel wall images on 2 different levels showing smooth, healthy vessel wall (**arrows**) and thickening and enhancement of the vessel wall of the right M1(**arrowheads**), indicative of cerebral vasculitis.

imaging rather easily, as has been shown by multiple studies.[11–14,17,20,21,29,31,33–35,40,42,44,45,47–50] With intracranial vessel wall imaging, multiple lesions in multiple segments often are detected that give a picture of the total burden of intracranial atherosclerosis. Detection and characterization of individual small intracranial vascular lesions may provide additional information (Figure 2). Plaques may be characterized by their location and shape. Similar to the rest of the arterial vasculature, there also may be a preferential location of intracranial atherosclerotic lesions. Although this location needs to be established, it can be hypothesized that a preferential location at the bifurcations of the different arteries exists similar to the rest of the arterial vasculature.[60] With respect to the shape of the arterial lesions, it is expected that when the resolution of intracranial vessel wall imaging is sufficient (≤0.5 mm^3), different subtypes of atherosclerotic plaques can be distinguished from complete concentric (around the arterial lumen) to more focal and eccentric on 1 side of the lumen of an intracranial arterial segment.[61] Still, only eccentric atherosclerotic plaques have been observed so far.[42,46,47] Furthermore, the size of the lesions and irregularity might be assessed. To do so, the presence of atherosclerotic lesions may be combined with the assessment of the arterial wall thickness and possible remodeling of the arterial lumen at the side of the lesion.

Vessel Wall (Lesion) Enhancement

With improvement of intracranial vessel wall imaging methods, recent studies have shown enhancement of smaller atherosclerotic plaques in intracranial vessels (Table 1).[9–12,32,38,41–43,46,47,51] MRI methods for contrast enhancement typically rely on the use of T1-weighted sequences. Contrast-enhanced sequences benefit from a strong effect of the gadolinium-based contrast agents as a result of T1 shortening caused by the contrast uptake. This will result in higher signal intensity on these T1-weighted MRI sequences when contrast is taken up by the vessel wall or plaque (Figure 1). For the detection of enhancement, an additional T1-weighted MRI sequence without contrast (precontrast) is used to compare with the contrast-enhanced sequence (postcontrast). Still, the added value of both precontrast and postcontrast T1-weighted sequences for the detection of intracranial vessel wall enhancement has not yet been established. When the enhancement is very clear such as with vasculitis, a postcontrast scan may be sufficient (Figures 3 and 4).[18,19,22] However, the contrast enhancement can also be modest, or intracranial vessel wall lesions may already have a relatively hyperintense signal before the administration of contrast (Figure 2).[9] In these more difficult cases, precontrast and postcontrast MRI vessel wall imaging is required to establish the presence of contrast uptake. Whether there is an optimal time point between contrast administration and peak enhancement needs to be determined. Preliminary results from 7 T MRI examinations show a contrast-to-noise ratio peak after 20 minutes of contrast administration (Figure 4). However, this needs to be established in a larger group of patients and might vary between individual cases and pathologies. Finally, the exact pathophysiological mechanisms of contrast uptake in the intracranial arterial walls and atherosclerotic plaques need to be established. These mechanisms may differ on the basis of the kind of pathology (eg, vasculitis, atherosclerotic plaque) imaged. Contrast enhancement may occur with more generalized or focal inflammation of the vessel wall, together with neovascularization and endothelial contrast leakage,[62] or as a result of vasa vasorum in atherosclerotic plaques. For instance, pathological enhancement of a plaque in a vessel supplying a stroke territory has been observed within 4 weeks of ischemic stroke, and the strength and presence of enhancement are closely related to the time between stroke and vessel wall assessment.[41] The degree of enhancement is thought to be closely correlated with the level of inflammatory activity, presumably as a result of neovascularization and increased endothelial permeability.[63]

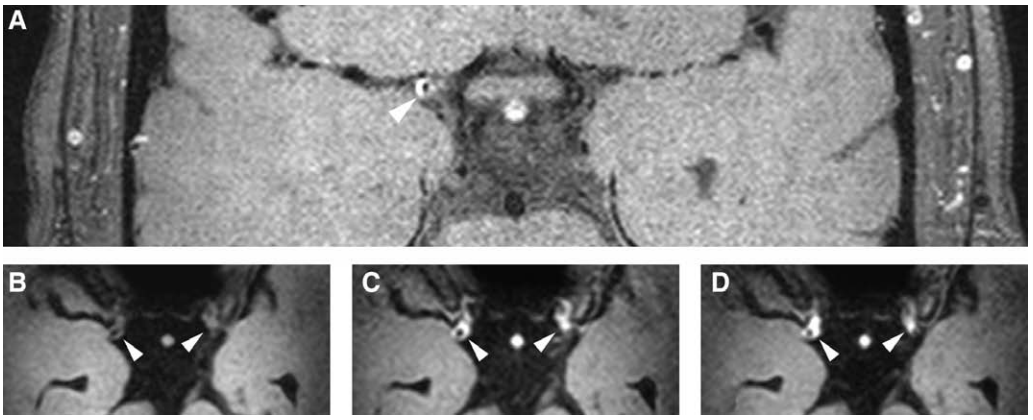

Figure 4. A 39-year-old woman presented with hemiparesis of the right arm and leg, headache, and aphasia caused by multiple ischemic infarcts in the left middle cerebral artery territory as seen on diffusion-weighted magnetic resonance images suspected of having Sneddon syndrome. **A**, Postcontrast 3 T, 3-dimensional, T1-weighted volumetric isotropic turbo spin-echo acquisition vessel wall image (sequence adjusted from Qiao et al;[20] repetition time/echo time, 1500/35 milliseconds) showing vessel wall enhancement of the right distal internal carotid artery (ICA). **B** through **D**, Corresponding 7 T, transverse, 3-dimensional magnetization preparation inversion recovery turbo spin-echo images before (**B**), directly after (**C**), and after 20 minutes (**D**) of contrast administration. **B**, Vessel wall lesions of the distal ICA on both sides. **C**, Enhancement of both the left and right distal ICA with even further enhancement after 20 minutes of contrast administration (**D**). The concentricity of the lesions and involvement of both ICAs can be indicative of moyamoya disease.

Vulnerable Plaques

Enhancing and nonenhancing plaques are classifications based on overt imaging characteristics, but a characteristic that is probably clinically more relevant is whether the plaque can be described as vulnerable. Vulnerable plaques, that is, atherosclerotic "active" plaques at risk for rupture, are associated with a high risk of (recurrent) ischemic events.[64] Similar to the characterization of carotid plaques, MRI might be used for the characterization of intracranial atherosclerotic plaques to assess the vulnerability of these plaques. For carotid plaques, plaque content differentiation includes the presence of calcifications, fibrin, lipid, vasa vasorum (plaque vascularization), and intraplaque hemorrhage.[64] Detection of intraplaque hemorrhage in particular was found to be related to a higher recurrent stroke risk.[65] In addition to plaque content, the presence of ulceration[66] and the size of the atherosclerotic plaque[67] were found to be correlated with prognosis. With further development of intracranial plaque imaging methods, we expect that characterization of the intracranial arterial plaque will also become possible in the next decade. Detection of intracranial plaque hemorrhage has already been shown to be possible intracranially[38,51] with an MR direct thrombus imaging[51] sequence for the middle cerebral artery (Table 1). In addition, several studies have investigated plaque vulnerability by means of contrast-enhanced sequences or used multiple contrast weightings (Figure 5).[10,32,38,41,42,68] Similar to black-blood techniques, the most successful MRI sequences for the detection of vulnerable plaque in the carotid arteries, for instance, MR direct thrombus imaging[51] combined with several image contrast weightings, should be optimized and tested for intracranial plaque characterization.

Clinical Implementation

In current clinical practice, it can be difficult to establish the cause of ischemic stroke in an individual patient, and differentiation between stroke subtypes is still an important issue.

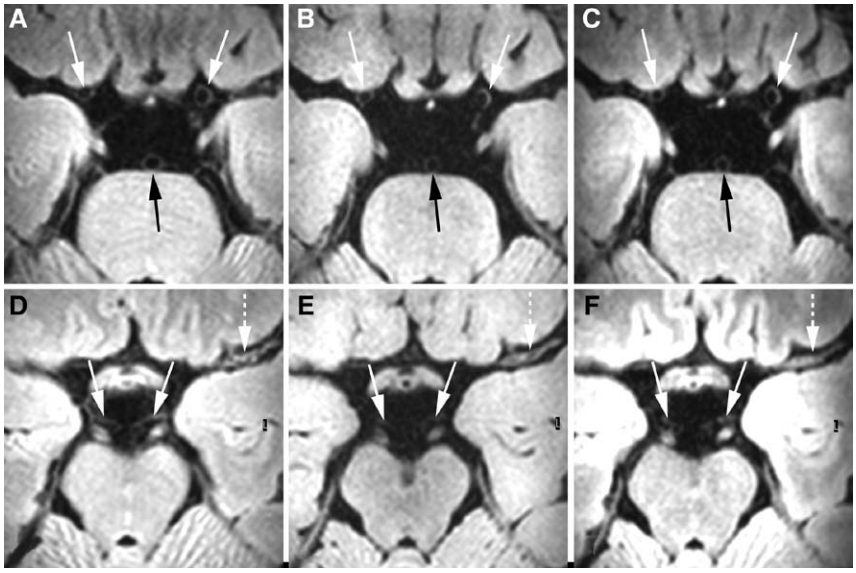

Figure 5. A 31-year-old man with moyamoya disease. A 7 T, 3-dimensional magnetization preparation inversion recovery turbo spin-echo (**A** and **D**) and whole-brain T1-weighted (**B** and **E**) and T2-weighted (**C** and **F**) magnetization preparation inversion recovery turbo spin-echo images. The vessel wall of the left internal carotid artery (ICA; (**white arrow** on the **right** in **A**–**C**) is slightly more hyperintense compared with the right ICA (**white arrow** on the **left** in **A**–**C**) and basilar artery (**black arrow** in **A**–**C**). Both distal ICAs are relatively narrow compared with the basilar artery. The left middle cerebral artery is seen to be almost occluded, with thickened vessel wall (**dashed arrow** in **D**–**F**). The normal P1 segment of the posterior cerebral artery can also be assessed (**white arrow** in **D**–**F**). Reproduced from van der Kolk et al[68] with kind permission of the publisher. Copyright © 2013 Springer Science+Business Media.

A method used to define the subtype of ischemic stroke is the Trial of Org 10172 in Acute Stroke Treatment (TOAST) classification system.[1] Stroke subtypes defined by this system are strokes with a large-artery atherosclerotic cause, cardioembolic strokes, small-artery strokes, strokes with a determined cause, and strokes with an undetermined cause. This classification system has limitations, with many stroke patients being diagnosed with an undetermined cause of stroke. Furthermore, in patients with a presumed cause of stroke, the certainty of the diagnosis often remains elusive. With the use of intracranial vessel wall imaging techniques, small changes within the vessel wall may be revealed, and the certainty of the diagnosis may become better established, enabling better therapeutic management.

In patients with ischemic stroke caused by large-artery atherosclerosis, intracranial vessel wall imaging may show more generalized atherosclerosis of the intracranial and extracranial vasculature, including the carotid arteries (Figure 6), vertebral arteries, and basilar artery. Furthermore, although lumenography may show complete recanalization, it can be hypothesized that small, flat nonstenotic remnants will still be present. In addition, it can also be hypothesized that an occlusive thromboembolus will give a local inflammatory reaction of the vessel wall at the point of occlusion, which may be visible on follow-up as a small area of scar tissue, which may decrease over time.

In the small-vessel occlusion group, intracranial vessel wall MR sequences may be able to differentiate between different causes of small subcortical infarcts by the visualization of the location of the occlusion, the severity of atherosclerosis, or the visualization of a possible thrombus in the trajectory of a probable occluded perforating artery.[69] On the other hand, small-artery atherosclerosis of the perforating artery itself may be difficult to assess if a thrombus is absent, although indirect characteristics such as small hemorrhagic changes in the penetrating artery[70] may prove to be of additional value.

Figure 6. A 52-year-old woman presented with disturbed balance and hemiparesis of the left arm and leg caused by infarctions of the right anterior cerebral artery, right middle cerebral artery, and right posterior cerebral artery, as seen on diffusion-weighted magnetic resonance images (not shown). Postcontrast 3 T, 3-dimensional, T1-weighted volumetric isotropic turbo spin-echo acquisition vessel wall image (sequence adjusted from Qiao et al[20] repetition time/echo time, 1500/35 milliseconds) showing an atherosclerotic plaque in the left distal internal carotid (**arrowhead**). On the basis of the plaque located in a large artery, this woman probably has large-artery atherosclerosis.

For ischemic strokes of other determined cause, intracranial vessel wall imaging may be of value by reducing the number of (sometimes very invasive) diagnostic studies needed to establish the diagnosis. In patients with vasculitis, for instance, the presence and severity of enhancement of the intracranial vessel wall may help establish the diagnosis[19] without the need of an elaborate diagnostic process and provide targeted treatment. It may also show early signs of the disease process and changes at follow-up, which enables fast treatment before serious ischemic events occur. In the remaining patients (≈40%), the cause of cerebral ischemia is unknown. Recent developments in intracranial vessel wall imaging may help to unravel their cause by showing the presence of vessel wall thickening and plaques and enhancement of plaques or vessel wall. In younger patients, uncommon causes of stroke such as dissections, vasculitis, and transient cerebral arteriopathy may be found to be the cause of stroke. Furthermore, the absence of atherosclerotic changes may favor a cardioembolic cause. In the acute phase, characterization of different underlying components of the plaque, embolic material, and thrombus material may give possibilities to guide and differentiate between stroke subtypes in this early stage. Intracranial vessel wall imaging may thus be a useful tool for identifying the causes of stroke. Moreover, for the therapeutic management of the individual patient, it is essential to determine the underlying cause of ischemic stroke. Antithrombotic medication or oral anticoagulants and lipid-lowering medication are standard treatment for the majority of ischemic stroke patients and are based on lowering the chance of developing subsequent (thrombo)emboli.[71] Common, more cause-specific treatment options include, among others, oral antiarrhythmic medication and atherosclerotic plaque removal (endarterectomy) or endovascular stenting for carotid artery stenosis.[71] Inflammatory vasculopathies such as vasculitis require intensive monitoring and aggressive treatment with immunosuppressive agents or, in the case of an infective cause, with antibiotics.[72] Furthermore, recent results of the Stenting and Aggressive Medical Management for Preventing Recurrent Stroke in Intracranial Stenosis (SAMMPRIS) trial showed that aggressive medical management, including dual antiplatelets, and lifestyle changes reduced future stroke risk in patients with intracranial stenosis[73] compared with previous studies[74] in similar populations. With the use of intracranial vessel wall imaging, the best treatment option may be determined earlier, preventing unnecessary treatment or wrong treatment, which might even jeopardize a patient's life. It would therefore be ideal to include a vessel wall sequence in the clinical scan protocol besides the regular clinical scans for ischemic stroke.

The following recommendations are made. First, if intracranial atherosclerosis is considered, a precontrast and postcontrast T1-weighted vessel wall sequence is recommended for investigating vulnerable plaques. Second, a postcontrast T1-weighted sequence can be used to detect diffuse vessel wall enhancement when acute cerebral vasculitis is expected. Third, for patients with transient ischemic attacks, a protocol including a T1-weighted vessel wall sequence before and after contrast administration for the identification of smaller lesions is recommended. Fourth, for plaque

characterization, multiple contrast weightings improve the detection of plaque components.

An overview of expected vessel wall abnormalities for different causes of ischemic stroke can be found in Table 2.

Future Directions

We are still in the early days of intracranial vessel wall imaging. We expect that the developments and applications of intracranial vessel wall imaging will follow a route similar to that for extracranial vessel wall and plaque imaging of the carotid artery. Ideally, MRI of the intracranial vessel wall should be able to describe the presence of both large and small (atherosclerotic) lesions and to characterize the lesions with respect to enhancement, plaque content, and vulnerability. However, at this moment, the lack of validation of MRI with histology to demonstrate the feasibility of intracranial vessel wall MRI in characterizing plaque components makes it difficult to establish the origin of the lesion on the basis of in vivo data only. For the extracranial arteries, histological validation is already widely available because carotid specimens are obtained with endarterectomy[75,76] and the in vivo MRI can be performed before surgery. For intracranial arteries, however, only a few studies addressed this issue.[36,53] The reason is that histological validations are difficult to perform because there are no current treatment options such as endarterectomy for the intracranial arteries. This histological validation is important for further development of in vivo imaging; therefore, future research should also focus on pathological validation of intracranial vessel wall imaging with, for instance, postmortem specimens of the circle of Willis. The complete assessment of the intracranial vasculature for atherosclerotic lesions may allow the identification and classification of culprit lesions. The detection and characterization of intracranial atherosclerotic lesions may further enhance our knowledge about intracranial atherosclerosis. In patients with an unknown cause of stroke (≈40%), intracranial vessel wall and plaque imaging may help to establish the cause of stroke. In patients with a probable or possible cause of stroke, information about the intracranial vessel wall, plaque, and other vascular fingerprints may further confirm the cause of stroke or might change the stroke classification. In addition to ischemic stroke, intracranial vessel wall imaging might also be used for other indications such as patients with a hemorrhagic stroke or patients with expected vascular dementia. For example, in patients with a subarachnoid hemorrhagic stroke and multiple aneurysms, enhancement detected with vessel wall imaging was found to be capable of identifying the symptomatic aneurysm.[39] In patients suspected to have vascular dementia, intracranial vessel wall imaging might contribute to a better understanding of the underlying vessel wall pathology, which may lead to better-tailored therapy for these patients. In general, a detailed and robust assessment of the intracranial vessel walls and plaque status might be used in follow-up studies to assess the progression over time and the potential effect of this progression on new medication.

Table 2. Intracranial Vessel Wall Abnormalities Expected for TOAST Stroke Subtypes

Stroke Subtype	Vessel Wall Abnormalities
Large-artery atherosclerosis	Small, flat nonstenotic remnants for the thrombus
	Enhancement of the vessel wall lesion
	Small intracranial atherosclerotic changes
	>50% stenosis
Small vessel occlusion	Enhancement at location of occlusion
	Possible thrombus
	Plaques related to proximal occlusion of perforating artery
Stroke of other determined cause	Early signs of vessel wall enhancement
	Plaques (without luminal stenosis)
	No cardiac sources or large-artery atherosclerosis
	Vessel wall enhancement (eg, vasculitis)
Stroke of undetermined cause	Presence of intracranial atherosclerosis
	Plaques
	Enhancement of the plaque
	Vessel wall enhancement

TOAST indicates Trial of Org 10172 in Acute Stroke Treatment.

Conclusions

MR intracranial vessel wall imaging is a fast growing area of clinical and scientific interest. With intracranial atherosclerosis being an important cause of stroke, intracranial vessel wall imaging will become more important despite the fact that the methodology requires further development. In the next decade, technical innovations and clinical applications within this field will result in new insights into the cause of stroke in individual patients, which might ultimately translate into better and more individualized stroke treatment.

Search Strategy and Selection Criteria

References for this review were identified through a search of PubMed between March 1968 and January 2014 and references from relevant articles. The search terms brain diseases, intracranial ischemia, stroke, intracranial arterial arteriosclerosis, cerebral arteries, intracranial vessel wall, and MRI were used. Only articles in English were reviewed. The final reference list was generated on the basis of relevance to the topics covered in this review.

Disclosures

None.

References

1. Adams HP Jr, Bendixen BH, Kappelle LJ, Biller J, Love BB, Gordon DL, Marsh EE 3rd. Classification of subtype of acute ischemic stroke: definitions for use in a multicenter clinical trial: TOAST: Trial of Org 10172 in Acute Stroke Treatment. *Stroke*. 1993;24:35–41.
2. Bash S, Villablanca JP, Jahan R, Duckwiler G, Tillis M, Kidwell C, Saver J, Sayre J. Intracranial vascular stenosis and occlusive disease: evaluation with CT angiography, MR angiography, and digital subtraction angiography. *AJNR Am J Neuroradiol*. 2005;26:1012–1021.
3. Kiechl S, Willeit J. The natural course of atherosclerosis, part II: vascular remodeling. *Arterioscler Thromb Vasc Biol*. 1999;19:1491–1498.

4. Glagov S, Weisenberg E, Zarins CK, Stankunavicius R, Kolettis GJ. Compensatory enlargement of human atherosclerotic coronary arteries. *N Engl J Med*. 1987;316:1371–1375.
5. Mandell DM, Shroff M. On MR imaging of the intracranial vessel wall. *Can J Neurol Sci*. 2011;38:4–5.
6. Mühlenbruch G, Das M, Mommertz G, Schaaf M, Langer S, Mahnken AH, Wildberger JE, Thron A, Günther RW, Krings T. Comparison of dual-source CT angiography and MR angiography in preoperative evaluation of intra- and extracranial vessels: a pilot study. *Eur Radiol*. 2010;20:469–476.
7. Arenillas JF. Intracranial atherosclerosis: current concepts. *Stroke*. 2011;42(suppl):S20–S23.
8. Qureshi AI, Caplan LR. Intracranial atherosclerosis. *Lancet*. 2013;6736:1–15.
9. van der Kolk AG, Zwanenburg JJ, Brundel M, Biessels GJ, Visser F, Luijten PR, Hendrikse J. Intracranial vessel wall imaging at 7.0-T MRI. *Stroke*. 2011;42:2478–2484.
10. Lou X, Ma N, Ma L, Jiang WJ. Contrast-enhanced 3T high-resolution MR imaging in symptomatic atherosclerotic basilar artery stenosis. *AJNR Am J Neuroradiol*. 2013;34:513–517.
11. Ma N, Jiang WJ, Lou X, Ma L, Du B, Cai JF, Zhao TQ. Arterial remodeling of advanced basilar atherosclerosis: a 3-Tesla MRI study. *Neurology*. 2010;75:253–258.
12. Ma N, Lou X, Zhao TQ, Wong EH, Jiang WJ. Intraobserver and interobserver variability for measuring the wall area of the basilar artery at the level of the trigeminal ganglion on high-resolution MR images. *AJNR Am J Neuroradiol*. 2011;32:E29–E32.
13. Park JK, Kim SH, Kim BS, Choi G, Jeong SY, Choi JC. Imaging of intracranial plaques with black-blood double inversion recovery MR imaging and CT. *J Neuroimaging*. 2011;21:e64–e68.
14. Chung GH, Kwak HS, Hwang SB, Jin GY. High resolution MR imaging in patients with symptomatic middle cerebral artery stenosis. *Eur J Radiol*. 2012;81:4069–4074.
15. Kim JM, Jung KH, Sohn CH, Moon J, Han MH, Roh JK. Middle cerebral artery plaque and prediction of the infarction pattern. *Arch Neurol*. 2012;69:1470–1475.
16. Kim YS, Lim SH, Oh KW, Kim JY, Koh SH, Kim J, Heo SH, Chang DI, Lee YJ, Kim HY. The advantage of high-resolution MRI in evaluating basilar plaques: a comparison study with MRA. *Atherosclerosis*. 2012;224:411–416.
17. Mi Kim S, Ryu CW, Jahng GH, Jong Kim E, Suk Choi W. Two different morphologies of chronic unilateral middle cerebral artery occlusion: evaluation using high-resolution MRI [published online ahead of print January 16, 2013]. *J Neuroimaging*. doi: 10.1111/jon.12009. http://onlinelibrary.wiley.com/doi/10.1111/jon.12009/abstract;jsessionid=3660FCB7B0B6D764E13E30AC535D8BCA.f03t04. Accessed June 20, 2013.
18. Mandell DM, Matouk CC, Farb RI, Krings T, Agid R, terBrugge K, Willinsky RA, Swartz RH, Silver FL, Mikulis DJ. Vessel wall MRI to differentiate between reversible cerebral vasoconstriction syndrome and central nervous system vasculitis: preliminary results. *Stroke*. 2012;43:860–862.
19. Pfefferkorn T, Linn J, Habs M, Opherk C, Cyran C, Ottomeyer C, Straube A, Dichgans M, Nikolaou K, Saam T. Black blood MRI in suspected large artery primary angiitis of the central nervous system. *J Neuroimaging*. 2013;23:379–383.
20. Qiao Y, Steinman DA, Qin Q, Etesami M, Schär M, Astor BC, Wasserman BA. Intracranial arterial wall imaging using three-dimensional high isotropic resolution black blood MRI at 3.0 Tesla. *J Magn Reson Imaging*. 2011;34:22–30.
21. Ryu CW, Jahng GH, Kim EJ, Choi WS, Yang DM. High resolution wall and lumen MRI of the middle cerebral arteries at 3 Tesla. *Cerebrovasc Dis*. 2009;27:433–442.
22. Saam T, Habs M, Pollatos O, Cyran C, Pfefferkorn T, Dichgans M, Dietrich O, Glaser C, Reiser MF, Nikolaou K, Nikolauo K. High-resolution black-blood contrast-enhanced T1 weighted images for the diagnosis and follow-up of intracranial arteritis. *Br J Radiol*. 2010;83:e182–e184.
23. Edelman RR, Chien D, Kim D. Fast selective black blood MR imaging. *Radiology*. 1991;181:655–660.
24. Koktzoglou I, Kirpalani A, Carroll TJ, Li D, Carr JC. Dark-blood MRI of the thoracic aorta with 3D diffusion-prepared steady-state free precession: initial clinical evaluation. *AJR Am J Roentgenol*. 2007;189:966–972.
25. Wang J, Yarnykh VL, Hatsukami T, Chu B, Balu N, Yuan C. Improved suppression of plaque-mimicking artifacts in black-blood carotid atherosclerosis imaging using a multislice motion-sensitized driven-equilibrium (MSDE) turbo spin-echo (TSE) sequence. *Magn Reson Med*. 2007;58:973–981.
26. Botnar RM, Stuber M, Kissinger KV, Kim WY, Spuentrup E, Manning WJ. Noninvasive coronary vessel wall and plaque imaging with magnetic resonance imaging. *Circulation*. 2000;102:2582–2587.
27. Aoki S, Shirouzu I, Sasaki Y, Okubo T, Hayashi N, Machida T, Hoshi E, Suzuki K, Funada N, Araki T. Enhancement of the intracranial arterial wall at MR imaging: relationship to cerebral atherosclerosis. *Radiology*. 1995;194:477–481.
28. Aoki S, Hayashi N, Abe O, Shirouzu I, Ishigame K, Okubo T, Nakagawa K, Ohtomo K, Araki T. Radiation-induced arteritis: thickened wall with prominent enhancement on cranial MR images report of five cases and comparison with 18 cases of Moyamoya disease. *Radiology*. 2002;223:683–688.
29. Klein IF, Lavallée PC, Mazighi M, Schouman-Claeys E, Labreuche J, Amarenco P. Basilar artery atherosclerotic plaques in paramedian and lacunar pontine infarctions: a high-resolution MRI study. *Stroke*. 2010;41:1405–1409.
30. Küker W, Gaertner S, Nagele T, Dopfer C, Schoning M, Fiehler J, Rothwell PM, Herrlinger U. Vessel wall contrast enhancement: a diagnostic sign of cerebral vasculitis. *Cerebrovasc Dis*. 2008;26:23–29.
31. Natori T, Sasaki M, Miyoshi M, Ohba H, Katsura N, Yamaguchi M, Narumi S, Kabasawa H, Kudo K, Ito K, Terayama Y. Evaluating middle cerebral artery atherosclerotic lesions in acute ischemic stroke using magnetic resonance T1-weighted 3-dimensional vessel wall imaging. *J Stroke Cerebrovasc Dis*. 2014;23:706–711.
32. Vakil P, Vranic J, Hurley MC, Bernstein RA, Korutz AW, Habib A, Shaibani A, Dehkordi FH, Carroll TJ, Ansari SA. T1 gadolinium enhancement of intracranial atherosclerotic plaques associated with symptomatic ischemic presentations. *AJNR Am J Neuroradiol*. 2013;34:2252–2258.
33. Klein IF, Lavallée PC, Touboul PJ, Schouman-Claeys E, Amarenco P. In vivo middle cerebral artery plaque imaging by high-resolution MRI. *Neurology*. 2006;67:327–329.
34. Klein IF, Lavallée PC, Schouman-Claeys E, Amarenco P. High-resolution MRI identifies basilar artery plaques in paramedian pontine infarct. *Neurology*. 2005;64:551–552.
35. Lam WW, Wong KS, So NM, Yeung TK, Gao S. Plaque volume measurement by magnetic resonance imaging as an index of remodeling of middle cerebral artery: correlation with transcranial color Doppler and magnetic resonance angiography. *Cerebrovasc Dis*. 2004;17:166–169.
36. Chen XY, Lam WW, Ng HK, Zhao HL, Wong KS. Diagnostic accuracy of MRI for middle cerebral artery stenosis: a postmortem study. *J Neuroimaging*. 2006;16:318–322.
37. Sparing R, Harrer JU, Spuentrup E, Krings T. MR-imaging of thrombus in extra- and intracranial arteries employing balanced fast-field echo MRI. *Neuroradiology*. 2004;46:973–977.
38. Chung JW, Kim BJ, Choi BS, Sohn CH, Bae HJ, Yoon BW, Lee SH. High-resolution magnetic resonance imaging reveals hidden etiologies of symptomatic vertebral arterial lesions. *J Stroke Cerebrovasc Dis*. 2014;23:293–302.
39. Matouk CC, Mandell DM, Günel M, Bulsara KR, Malhotra A, Hebert R, Johnson MH, Mikulis DJ, Minja FJ. Vessel wall magnetic resonance imaging identifies the site of rupture in patients with multiple intracranial aneurysms: proof of principle. *Neurosurgery*. 2013;72:492–496.
40. Shi M, Wang S, Zhou H, Cheng Y, Feng J, Wu J. Wingspan stenting of symptomatic middle cerebral artery stenosis and perioperative evaluation using high-resolution 3 Tesla MRI. *J Clin Neurosci*. 2012;19:912–914.
41. Skarpathiotakis M, Mandell DM, Swartz RH, Tomlinson G, Mikulis DJ. Intracranial atherosclerotic plaque enhancement in patients with ischemic stroke. *AJNR Am J Neuroradiol*. 2013;34:299–304.
42. Swartz RH, Bhuta SS, Farb RI, Agid R, Willinsky RA, Terbrugge KG, Butany J, Wasserman BA, Johnstone DM, Silver FL, Mikulis DJ. Intracranial arterial wall imaging using high-resolution 3-Tesla contrast-enhanced MRI. *Neurology*. 2009;72:627–634.
43. Turan TN, Rumboldt Z, Brown TR. High-resolution MRI of basilar atherosclerosis: three-dimensional acquisition and FLAIR sequences. *Brain Behav*. 2013;3:1–3.
44. Xu WH, Li ML, Gao S, Ni J, Zhou LX, Yao M, Peng B, Feng F, Jin ZY, Cui LY. In vivo high-resolution MR imaging of symptomatic and asymptomatic middle cerebral artery atherosclerotic stenosis. *Atherosclerosis*. 2010;212:507–511.
45. Xu WH, Li ML, Gao S, Ni J, Zhou LX, Yao M, Peng B, Feng F, Jin ZY, Cui LY. Plaque distribution of stenotic middle cerebral artery and its clinical relevance. *Stroke*. 2011;42:2957–2959.
46. Vergouwen MD, Silver FL, Mandell DM, Mikulis DJ, Krings T, Swartz RH. Fibrous cap enhancement in symptomatic atherosclerotic basilar artery stenosis. *Arch Neurol*. 2011;68:676.

47. Vergouwen MD, Silver FL, Mandell DM, Mikulis DJ, Swartz RH. Eccentric narrowing and enhancement of symptomatic middle cerebral artery stenoses in patients with recent ischemic stroke. *Arch Neurol*. 2011;68:338–342.
48. Li ML, Xu WH, Song L, Feng F, You H, Ni J, Gao S, Cui LY, Jin ZY. Atherosclerosis of middle cerebral artery: evaluation with high-resolution MR imaging at 3T. *Atherosclerosis*. 2009;204:447–452.
49. Niizuma K, Shimizu H, Takada S, Tominaga T. Middle cerebral artery plaque imaging using 3-Tesla high-resolution MRI. *J Clin Neurosci*. 2008;15:1137–1141.
50. Zhu XJ, Du B, Lou X, Hui FK, Ma L, Zheng BW, Jin M, Wang CX, Jiang WJ. Morphologic characteristics of atherosclerotic middle cerebral arteries on 3T high-resolution MRI. *AJNR Am J Neuroradiol*. 2013;34:1717–1722.
51. Turan TN, Bonilha L, Morgan PS, Adams RJ, Chimowitz MI. Intraplaque hemorrhage in symptomatic intracranial atherosclerotic disease. *J Neuroimaging*. 2011;21:e159–e161.
52. van der Kolk AG, Hendrikse J, Zwanenburg JJ, Visser F, Luijten PR. Clinical applications of 7 T MRI in the brain. *Eur J Radiol*. 2013;82:708–718.
53. Majidi S, Sein J, Watanabe M, Hassan AE, Van de Moortele PF, Suri MF, Clark HB, Qureshi AI. Intracranial-derived atherosclerosis assessment: an in vitro comparison between virtual histology by intravascular ultrasonography, 7T MRI, and histopathologic findings. *AJNR Am J Neuroradiol*. 2013;34:2259–2264.
54. Marinković S, Gibo H, Milisavljević M. The surgical anatomy of the relationships between the perforating and the leptomeningeal arteries. *Neurosurgery*. 1996;39:72–83.
55. Kamath S. Observations on the length and diameter of vessels forming the circle of Willis. *J Anat*. 1981;133(pt 3):419–423.
56. Haacke M. *Magnetic Resonance Imaging: Physical Principles and Sequence Design*. New York, NY: Wiley-Liss; 1999.
57. Chen XY, Wong KS, Lam WW, Zhao HL, Ng HK. Middle cerebral artery atherosclerosis: histological comparison between plaques associated with and not associated with infarct in a postmortem study. *Cerebrovasc Dis*. 2008;25:74–80.
58. Duivenvoorden R, de Groot E, Elsen BM, Laméris JS, van der Geest RJ, Stroes ES, Kastelein JJ, Nederveen AJ. In vivo quantification of carotid artery wall dimensions: 3.0-Tesla MRI versus B-mode ultrasound imaging. *Circ Cardiovasc Imaging*. 2009;2:235–242.
59. Touboul PJ, Elbaz A, Koller C, Lucas C, Adraï V, Chédru F, Amarenco P. Common carotid artery intima-media thickness and brain infarction: the Etude du Profil Génétique de l'Infarctus Cérébral (GENIC) case-control study: the GENIC Investigators. *Circulation*. 2000;102:313–318.
60. Ravensbergen J, Ravensbergen JW, Krijger JK, Hillen B, Hoogstraten HW. Localizing role of hemodynamics in atherosclerosis in several human vertebrobasilar junction geometries. *Arterioscler Thromb Vasc Biol*. 1998;18:708–716.
61. Honye J, Mahon DJ, Jain A, White CJ, Ramee SR, Wallis JB, al-Zarka A, Tobis JM. Morphological effects of coronary balloon angioplasty in vivo assessed by intravascular ultrasound imaging. *Circulation*. 1992;85:1012–1025.
62. Sluimer JC, Kolodgie FD, Bijnens AP, Maxfield K, Pacheco E, Kutys B, Duimel H, Frederik PM, van Hinsbergh VW, Virmani R, Daemen MJ. Thin-walled microvessels in human coronary atherosclerotic plaques show incomplete endothelial junctions relevance of compromised structural integrity for intraplaque microvascular leakage. *J Am Coll Cardiol*. 2009;53:1517–1527.
63. Qiao Y, Etesami M, Astor BC, Zeiler SR, Trout HH 3rd, Wasserman BA. Carotid plaque neovascularization and hemorrhage detected by MR imaging are associated with recent cerebrovascular ischemic events. *AJNR Am J Neuroradiol*. 2012;33:755–760.
64. Saam T, Hatsukami TS, Takaya N, Chu B, Underhill H, Kerwin WS, Cai J, Ferguson MS, Yuan C. The vulnerable, or high-risk, atherosclerotic plaque: noninvasive MR imaging for characterization and assessment. *Radiology*. 2007;244:64–77.
65. Virmani R, Kolodgie FD, Burke AP, Finn AV, Gold HK, Tulenko TN, Wrenn SP, Narula J. Atherosclerotic plaque progression and vulnerability to rupture: angiogenesis as a source of intraplaque hemorrhage. *Arterioscler Thromb Vasc Biol*. 2005;25:2054–2061.
66. Edwards JH, Kricheff II, Riles T, Imparato A. Angiographically undetected ulceration of the carotid bifurcation as a cause of embolic stroke. *Radiology*. 1979;132:369–373.
67. Yuan C, Mitsumori LM, Beach KW, Maravilla KR. Carotid atherosclerotic plaque: noninvasive MR characterization and identification of vulnerable lesions. *Radiology*. 2001;221:285–299.
68. van der Kolk AG, Hendrikse J, Brundel M, Biessels GJ, Smit EJ, Visser F, Luijten PR, Zwanenburg JJ. Multi-sequence whole-brain intracranial vessel wall imaging at 7.0 Tesla. *Eur Radiol*. 2013;23:2996–3004.
69. Wardlaw JM, Dennis MS, Warlow CP, Sandercock PA. Imaging appearance of the symptomatic perforating artery in patients with lacunar infarction: occlusion or other vascular pathology? *Ann Neurol*. 2001;50:208–215.
70. Biessels GJ, Zwanenburg JJ, Visser F, Frijns CJ, Luijten PR. Hypertensive cerebral hemorrhage: imaging the leak with 7-T MRI. *Neurology*. 2010;75:572–573.
71. Furie KL, Kasner SE, Adams RJ, Albers GW, Bush RL, Fagan SC, Halperin JL, Johnston SC, Katzan I, Kernan WN, Mitchell PH, Ovbiagele B, Palesch YY, Sacco RL, Schwamm LH, Wassertheil-Smoller S, Turan TN, Wentworth D; American Heart Association Stroke Council, Council on Cardiovascular Nursing, Council on Clinical Cardiology, Interdisciplinary Council on Quality of Care and Outcomes Research. Guidelines for the prevention of stroke in patients with stroke or transient ischemic attack: a guideline for healthcare professionals from the American Heart Association/American Stroke Association. *Stroke*. 2011;42:227–276.
72. Hajj-Ali RA, Singhal AB, Benseler S, Molloy E, Calabrese LH. Primary angiitis of the CNS. *Lancet Neurol*. 2011;10:561–572.
73. Derdeyn CP, Chimowitz MI, Lynn MJ, Fiorella D, Turan TN, Janis LS, Montgomery J, Nizam A, Lane BF, Lutsep HL, Barnwell SL, Waters MF, Hoh BL, Hourihane JM, Levy EI, Alexandrov AV, Harrigan MR, Chiu D, Klucznik RP, Clark JM, McDougall CG, Johnson MD, Pride GL, Lynch JR, Zaidat OO, Rumboldt Z, Cloft HJ. Aggressive medical treatment with or without stenting in high-risk patients with intracranial artery stenosis (SAMMPRIS): the final results of a randomised trial. *Lancet*. 2013;6736:1–9.
74. Chimowitz MI, Lynn MJ, Howlett-Smith H, Stern BJ, Hertzberg VS, Frankel MR, Levine SR, Chaturvedi S, Kasner SE, Benesch CG, Sila CA, Jovin TG, Romano JG; Warfarin-Aspirin Symptomatic Intracranial Disease Trial Investigators. Comparison of warfarin and aspirin for symptomatic intracranial arterial stenosis. *N Engl J Med*. 2005;352:1305–1316.
75. Yuan C, Hatsukami TS, Obrien KD. High-resolution magnetic resonance imaging of normal and atherosclerotic human coronary arteries ex vivo: discrimination of plaque tissue components. *J Investig Med*. 2001;49:491–499.
76. den Hartog AG, Bovens SM, Koning W, Hendrikse J, Luijten PR, Moll FL, Pasterkamp G, de Borst GJ. Current status of clinical magnetic resonance imaging for plaque characterisation in patients with carotid artery stenosis. *Eur J Vasc Endovasc Surg*. 2013;45:7–21.

KEY WORDS: infarction ■ magnetic resonance imaging ■ neuroimaging ■ plaque, atherosclerotic ■ stroke

Imaging Intracranial Vessel Wall Pathology With Magnetic Resonance Imaging: Current Prospects and Future Directions

Nikki Dieleman, Anja G. van der Kolk, Jaco J.M. Zwanenburg, Anita A. Harteveld, Geert J. Biessels, Peter R. Luijten and Jeroen Hendrikse

Circulation. 2014;130:192-201
doi: 10.1161/CIRCULATIONAHA.113.006919
Circulation is published by the American Heart Association, 7272 Greenville Avenue, Dallas, TX 75231

Print ISSN: 0009-7322. Online ISSN: 1524-4539